

# Synergistic antibacterial action of the iron complex and ampicillin against *Staphylococcus aureus*

**Ludmila Kosaristanova**

Mendel University in Brno

**Martin Rihacek**

Mendel University in Brno

**Frantiska Sucha**

Mendel University in Brno

**Vedran Milosavljevic**

Mendel University in Brno

**Pavel Svec**

Mendel University in Brno

**Jana Dorazilova**

University of Technology

**Lucy Vojtova**

University of Technology

**Peter Antal**

Palacky University

**Pavel Kopel**

Palacky University

**Zdenek Patocka**

Mendel University in Brno

**Vojtech Adam**

Mendel University in Brno

**Ludek Zurek**

Mendel University in Brno

**Kristyna Dolezelikova** (✉ [kriki.cihalova@seznam.cz](mailto:kriki.cihalova@seznam.cz))

Mendel University in Brno

---

## Research Article

**Keywords:** *Staphylococcus aureus*, iron complex, ampicillin, synergy, antimicrobial activity

**Posted Date:** May 12th, 2023

**DOI:** <https://doi.org/10.21203/rs.3.rs-2906921/v1>

**License:**  This work is licensed under a Creative Commons Attribution 4.0 International License.

[Read Full License](#)

---

# Abstract

## Objectives

Resistance to antibiotics among bacteria of clinical importance, including *Staphylococcus aureus*, is a serious problem worldwide and the search for alternatives is needed. Some metal complexes have antibacterial properties and when combined with antibiotics, they may increase bacterial sensitivity to antimicrobials. In this study, we synthesized the iron complex and tested it in combination with ampicillin (Fe16 + AMP) against *S. aureus*.

## Methods

An iron complex (Fe16) was synthesized and characterized using spectroscopy methods. Confirmation of the synergistic effect between the iron complex (Fe16) and ampicillin (AMP) was performed using  $\zeta$ -potential, infrared spectra and FICI index calculated from minimum inhibitory concentration (MIC). Cytotoxic properties of combination Fe16 + AMP was evaluated on eukaryotic cell line. Impact of combination Fe16 + AMP on chosen genes of *S. aureus* were performed by Quantitative Real-Time PCR.

## Results

The MIC of Fe16 + AMP was significantly lower than that of AMP and Fe16 alone. Furthermore, the infrared spectroscopy revealed the change in the  $\zeta$ -potential of Fe16 + AMP. We demonstrated the ability of Fe16 + AMP to disrupt the bacterial membrane of *S. aureus* and that likely allowed for better absorption of AMP. In addition, the change in gene expression of bacterial efflux pumps at the sub-inhibitory concentration of AMP suggests an insufficient import of iron into the bacterial cell. At the same time, Fe16 + AMP did not have any cytotoxic effects on keratinocytes.

## Conclusions

Combined Fe16 + AMP therapy demonstrated significant synergistic and antimicrobial effects against *S. aureus*. This study supports the potential of combination therapy and further research.

## 1. Introduction

The emergence of antimicrobial resistance is a problem causing a global crisis and the rate of development of new antimicrobial agents is not adequate. Consequently, infections caused by multidrug-resistant bacteria including *Staphylococcus aureus* are of a great concern worldwide (1). Staphylococcal infections in humans and animals are commonly treated with  $\beta$ -lactam antibiotics, including ampicillin (AMP) (2). A great selective pressure from the intensive and extensive use of antibiotics has resulted in  $\beta$ -lactam resistance based on several mechanisms such as efflux pumps, siderophores, and production of  $\beta$ -lactamases (2–4). Currently, the majority of clinical strains of *S. aureus* are  $\beta$ -lactamase positive (2), use efflux pumps, and also produces siderophores (3, 4).

Antimicrobial properties of metals have been known for several decades (5) and their combination with antibiotics has been assessed in several studies. For example, it was shown that  $\beta$ -lactams together with silver or zinc oxide nanoparticles had great antimicrobial activity against various multidrug resistant bacteria (6, 7). Iron has been also considered as a potential candidate for combined treatment with antibiotics (8). Iron is the most abundant transition element in the human body and a promising antimicrobial agent in the form of a metal complex. Iron in the form of a metal complex can affect bacterial cells where they cause oxidative stress, inhibit respiratory processes and ATP production, increase cell hydrophobicity, and facilitate their penetration across the cell wall (7–9). Therefore, combined treatments offer several advantages such as a lower potential for developing resistance, additive or synergistic effects, increasing the effectivity of antibiotics, and overcoming drug resistance (10). Combination therapy of an iron complex with  $\beta$ -lactams has been tested previously against *Escherichia coli* and it was more effective than antibiotics alone (9).

The goal of this study was to synthesize the iron complex Fe16 and test it in combination with AMP against *S. aureus*. We also aimed to investigate the mechanism of the synergistic action of Fe16 + AMP against *S. aureus* and to evaluate whether it has any negative effects on eukaryotic cells represented by the HaCaT cell line.

## 2. Results

The infrared spectrum of Fe16 exhibited characteristic bands of the Fe(II)-tris(diimine) complexes. Also, the electronic spectra of Fe16 showed absorption bands characteristic for Fe(II)-tris(diimine) complexes (Fig. S1Aa,b and Table S2). Interactions between Fe16 and AMP were confirmed by the  $\zeta$ -potential and ATR-FTIR. The  $\zeta$ -potential of Fe16 alone was + 55.8 mV and AMP alone was - 16.5 mV. The  $\zeta$ -potential of Fe16 + AMP was shifted toward slightly negative values - 4.2 mV (Fig. S2) indicating the formation of new complexes. To further study the interactions between Fe16 and AMP in the Fe16 + AMP complex, spectra of Fe16, AMP, and Fe16 + AMP were recorded by ATR-FTIR (Fig. S1C). No major spectral alterations were observed comparing the Fe16 spectrum and the Fe16 subtracted spectra. With the focus on AMP and AMP subtracted spectra, the two significant band broadenings corresponding to valence carboxylate vibrations ( $\text{COO}^-$ ) at the wave number values of 1 590 and 1 370  $\text{cm}^{-1}$  were observed in spectrum of Fe16 + AMP. These c-carboxylate groups mediate the interaction in Fe16 + AMP complex.

The inhibitory effect of Fe16 + AMP against *S. aureus* was significantly greater than that of the individual compounds (Fig. 1A). The MIC value of Fe16 + AMP against *S. aureus* was significantly lower (0.5  $\mu\text{g/ml}$ ) than that of Fe16 and AMP alone with MIC values of 31.0  $\mu\text{g/ml}$  and 8.0  $\mu\text{g/ml}$ , respectively ( $p$ -value < 0.0001). The significant difference in MIC were detected between Fe16 and Fe16 + AMP groups and between AMP and Fe16 + AMP groups ( $p$ -value < 0.0001). This finding also correlated with the results of the FIC index. The antibacterial effect of the Fe16 + AMP and its synergistic effect ( $\leq 0.5$ ) against *S. aureus* was confirmed by the FIC index 0.1. SEM microscopy of *S. aureus* treated with Fe16 + AMP revealed that the integrity of the cell wall was compromised. In contrast, untreated *S. aureus* cells retained their coccus morphology and the cell surface was compact (Fig. 1Cb). In the cross-section, untreated *S.*

*aureus* cells showed typical cellular characteristics. On the other hand, significant morphological changes were observed after 24 h on *S. aureus* cells treated with Fe16 + AMP at the sub-inhibitory concentration (0.25 µg/ml) showing damaged cells with disrupted walls and membranes (Fig. 1Bb). The cytotoxic effect of Fe16 on the HaCaT keratinocyte cell line was observed in the concentration range of 8–125 µg/ml, whereas for AMP no cytotoxicity was observed (Fig. 1C). At the concentration of MIC 0.5 of Fe16 + AMP the viability of keratinocytes was 90.0% (Fig. 1C).

The expression of the efflux pump gene *mepA* significantly increased after all three treatments (fold change in the range 3.43–9.33) although the effect of AMP alone was at significance level  $p$ -value < 0.01. The expression of the *norA* gene also significantly increased after AMP (2.8 fold change) and Fe16 + AMP (3.1 fold change) treatments (Fig. 2A). Gene expression of *blaZ* was downregulated, although not significantly ( $p$ -value > 0.2) (Fig. 2A). The significantly increased expression was detected for the transporter genes *trpABC* and *fhuB* after exposure to Fe16 and Fe16 + AMP ( $p$ -value < 0.05) (Fig. 2B). Ampicillin alone affected the expression of *trpABC* only. The expression of the third ABC transporter gene, *htsA*, was downregulated non-significantly after all treatments (Table S3).

### 3. Discussion

In recent decades, many metal-based complexes have been tested for their antimicrobial properties (1, 8). It has been shown that iron exhibits antimicrobial effects against Gram-positive and Gram-negative bacteria in the form of metal complex or nanoparticles (8, 12).

In the synthesized complexes structure (13), the difference in wavelengths observed for asymmetric and symmetric  $\nu(\text{COO}^-)$  vibrations indicates that the compound Fe16 adopt ionic structure and fumarate ions are not coordinated to the central atoms. The strong bands can be assigned to asymmetric  $\nu(\text{COO}^-)$  vibrations but suffer interference with C = C and C = N stretching vibrations of aromatic ring (14). Considering that  $pK_a$  values of AMP functional groups (2.5/7.3) the carboxylic acid became anionic ( $\text{COO}^-$ ), and amine group cationic ( $\text{NH}_3^+$ ) (15). However, with increase the pH over the AMP  $pK_a$  values the targeted Fe16 complex after interaction with AMP became deprotonated (anionic form), which explains the strong decrease of the Fe16 complex positive charge and slight increase of negative surface charge of newly formed complexes. Due to the shift of carboxylate asymmetric valence vibrations to higher wavenumbers and symmetric valence vibration to lower numbers are observed in FTIR analysis. These spectral variations are connected to the carboxylate group passing from the free zwitterionic  $\text{COO}^-$  group to organometallic coordination in the Fe16 + AMP (16). The band shifts in spectral region suggest interaction of AMP phenyl with nphen in Fe16 via  $\pi$ - $\pi$  electron donor-acceptor complex system (17), while the vibration positions related to  $\beta$ -lactam ring in AMP as well as  $\text{NO}_2$  functional group in Fe16 remains unchanged. These data indicate that the key antibacterial structure in the complex remains unaffected (18).

The antimicrobial effect of Fe16 + AMP on *S. aureus* showed synergistic activity at three phenotypic and transcriptomic level. Previously, it was shown that other metals such as copper, zinc, and iron in

combination with amoxicillin increased effectiveness against *E. coli* (9). Although susceptibility of bacteria to doped antibiotics with metal complexes has been shown before (19), investigations on the iron complex are rare (8). Cell integrity of *S. aureus* treated with Fe16 + AMP was compromised leading to cell death which corroborates similar study with silver nanoparticles and antibiotics (20). Metal complexes increase the lipophilic character of the transition metal ion and therefore increase the hydrophobicity and facilitate their penetration through the bacterial cell wall and membrane (9). In our case, Fe16 + AMP appears to facilitate the penetration of AMP through the cell wall of *S. aureus*. Study of Panacek et al. (2016) showed that with AgNps silver nanoparticles in combination with antibiotics including beta-lactams had also synergistic effect against *S. aureus* (21).

It is important to note that no cytotoxic effects against the HaCaT cell line after exposure to Fe16 + AMP was observed. In recent years, many neurological disorders have been attributed to iron overload; however, further studies have optimized new complex metal compounds in combination with various materials to moderate general cytotoxicity (22, 23).

The combination of Fe16 + AMP at the sub-inhibitory concentration also likely led to disruption of the efflux pumps and that is consistent with the MICs results. The study of the inhibitory effect of efflux pumps under the influence of the iron complex alone and in combination with antibiotics has not been conducted previously. However, binding of iron oxide nanoparticles with rifampicin to the active site of the efflux pump and consequent blocking of its function has been demonstrated (24). Termination of the proton gradient, followed by disruption of the membrane potential and/or loss of proton motive force can lead to failure of the driving force, which is essential for the function of efflux pumps (25, 26). It is also assumed that iron nanoparticles disrupt the activity of efflux pumps by generating ROS (26). Large metal oxides have the ability to induce faster electron transfer kinetics to the active site of enzymes (27). Similarly, upregulation of *mepA* has been reported using silver nanoparticles and subsequent exposure to  $Ag^+$  ions (28). As the downregulation of *blaZ* was demonstrated, the association of antibiotics with metals suppresses  $\beta$ -lactamase hydrolase and therefore antibiotics can pass better through the bacterial cell wall (29). Another indicator of the instability of the defense system of *S. aureus* was a change in the gene expression of the ABC transporters. The overexpression of the ABC transporters under AMP treatment, in our case the *trpABC* gene, suggests rapid adaptation of the reactive immune system and elevation of uptake of iron into the cell which is consistent with the MIC results (30). On the other hand, the increased expression of *trpABC* and *fhuB* under the influence of Fe16 and Fe16 + AMP and the downregulation of *htsA* in all treatments indicate insufficient uptake of iron by the cell. Inactivation of intramembrane proteolysis of the ABC transporter was found to increase the susceptibility of *S. aureus* to several antimicrobial agents (31). In another study, the inhibitory effect of zinc on the metal uptake by the ABC transporters at physiological concentrations was demonstrated (32). However, the number of studies focused on this topic is low and further research is needed. Based on our results, we propose that the application of Fe16 + AMP causes stress in *S. aureus*, facilitates the penetration of AMP through the cell wall, and disrupts the function of efflux pumps and ABC transporters (Fig. 3). This together with insufficient iron intake leads to the bacterial cell death.

In conclusion, Fe16 + AMP is a promising new alternative for treatment of infections caused by *S. aureus* and potentially other pathogenic bacteria. Our results also demonstrate that this combination has no cytotoxic side effects on eukaryotic cells.

## 4. Methods

Ferric fumarate, H<sub>2</sub>fu = fumaric acid and 5-nitro-1,10-phenanthroline (nphen) (Sigma Aldrich, USA) were used for the synthesis of the Fe16= [Fe(nphen)<sub>3</sub>](fu)·7H<sub>2</sub>O complex. Iron fumarate was mixed in 40.0 ml of water with nphen dispersed in the same solvent and stirred for 6.0 h at 40.0°C. Characterization of Fe16, AMP and Fe16 + AMP was conducted by spectroscopic methods. The iron-antibiotic complex was prepared by mixing Fe16 with AMP in MilliQ water at a concentration of 1.0 mg/ml each and stirred at room temperature for 24 hours at 45 rpm. Synergistic effect between Fe16 and AMP was evaluated by the ζ-potential and infrared spectra (ATR-FTIR). Samples were subjected to analysis of DLS for ζ-potential. The Fourier transform infrared spectrometer equipped with a diamond crystal was used to record infrared spectra of Fe16, AMP and Fe16 + AMP via the attenuated total reflectance method (ATR-FTIR, Vertex 70v, Bruker, Billerica, MA, USA). Detailed methodology is described in the supplementary file.

*Staphylococcus aureus* CCM 4223 (Czech Collection of Microorganisms, Masaryk University, Brno, Czech Republic) was cultured on 5.0% Columbia blood agar (LMS, Czech Republic) at 37.0°C overnight. Antimicrobial activity of Fe16, AMP and Fe16 + AMP was tested by the minimum inhibitory concentration (MIC). *Staphylococcus aureus* was placed in 96-well microplates and Fe16, AMP, and Fe16 + AMP at the concentration range 0.125-31.0 µg/ml were added. MIC was determined by the Multiscan (Thermo Scientific, USA) at 37.0°C for 24 h. The absorbance reads at optical density 620 nm were monitored at 0 and 24 h. The interactions between Fe16 and AMP were quantitatively evaluated by the fractional inhibitory concentration index (FICI) calculated based on the formula (MIC of A in combination/MIC of A) + (MIC of B in combination/MIC of B) (11). Cytotoxic properties of Fe16, AMP, and Fe16 + AMP were evaluated by the spontaneously transformed aneuploidy immortal keratinocyte cell line from the adult human skin (HaCaT). Cell viability was quantified using the MTT assay. Cell morphology of *S. aureus* after Fe16 + AMP treatment was observed by SEM. *Staphylococcus aureus* was mixed with Fe16 + AMP in concentration 0.25 µg/ml and cultured at 37.0°C overnight. After incubation, samples were fixed by glutaraldehyde (1.0%) and incubated for 30 min at room temperature. Samples were then dehydrated using an ascending ethanol series in range 40–100% in several steps. Cell morphology was examined by SEM on the Tescan MAIA 3 equipped with a field emission gun (Tescan Ltd., Brno, Czech Republic). More detailed methods are in the supplementary file.

For RNA extraction, *S. aureus* was cultured overnight in Luria-Bertani (LB) broth at 37.0°C and shaking at 120 rpm with and without sub-inhibitory concentrations of 0.25 µg/ml for Fe16, AMP, and Fe16 + AMP. The RNA extraction was performed using TRIzol reagent® (TRIzol Reagent, Invitrogen, Carlsbad, CA) according to the manufacturer instructions. The isolated RNA was purified by ethanol RNA/DNA precipitation and reverse transcription was performed with the transcriptor first strand cDNA synthesis kit for RT-PCR (Roche, Mannheim, Germany) based on the manufacturer instructions using 500.0 ng RNA.

Quantitative real-time PCR analysis was performed using the qTOWER3 system (Analytik Jena, Jena, Germany) with *rpoB* as the housekeeping gene. Results were visualized as log<sub>2</sub> fold change ( $\Delta\Delta C_t$ ) calculations. All primers were designed using the IDT system. More detailed methods are in the supplementary file.

Results from MICs of biological triplicates and the differences between tested samples were analyzed by two-way ANOVA and Tukey's multiple comparison tests. The unpaired t-test between untreated and treated sample from  $\Delta C_t$  values of biological triplicate was used to determine the impact of treatments on defense system of *S. aureus*. All statistical analysis and graphical visualizations were done using GraphPad Prism 8.0.1. (GraphPad Software, CA, USA).

## Abbreviations

### **AMP**

Ampicillin

### **ATR-FTIR**

Attenuated total reflectance-Fourier-transform infrared spectroscopy

### **DLS**

Dynamic light scattering

### **Fe16**

Iron complex

### **Fe16 + AMP**

Combination of iron complex with ampicillin

### **FIC**

Fractional Inhibitory Concentration

### **MIC**

Minimum inhibitory concentration

### **RPM**

Revolutions per minute

## Declarations

*Ethics approval and consent to participate*

Not applicable.

*Competing interests*

The authors declare that they have no competing interests.

*Funding*



ERDF "Multidisciplinary research to increase application potential of nanomaterials in agricultural practice" and the CzechNanoLab project LM2018110 funded by MEYS CR.

### *Availability of data and materials*

Data is available on the department share drive and can be uploaded when requested. The first author may be contacted if someone wants to request the data from this study.

### *Consent to publish*

Not Applicable.

### *Authors' contributions*

PK and PA performed the synthesis and characterization of the iron complex and gave comments. LV, JD and VM did the experiments and evaluation with comments of the synergistic effect between the iron complex and ampicillins. FS performed the cytotoxicity experiment and PS SEM microscopy. MR designed experiment of Quantitative Real-Time PCR and evaluation of results. LK performed experiments, analyzed and commented microbiological and molecular parts and completion and writing of the article. ZP designed statistical evaluation. VA edited the manuscript. KD and LZ designed the project, supervised the experiments and wrote the report. All authors have read and approved the final manuscript.

### **Acknowledgments**

This work was supported by the ERDF "Multidisciplinary research to increase application potential of nanomaterials in agricultural practice" (No. CZ.02.1.01/0.0/0.0/16\_025/0007314). CzechNanoLab project LM2018110 funded by MEYS CR is acknowledged for the financial support of the measurements at CEITEC Nano Research Infrastructure.

### **References**

1. Nasiri Sovari S, Zobi F. Recent studies on the antimicrobial activity of transition metal complexes of groups 6–12. *Chemistry* 2020;2(2):418-52.
2. Teethaisong Y, Autarkool N, Sirichaiwetchakoon K, Krubphachaya P, Kupittayanant S, Eumkeb G. Synergistic activity and mechanism of action of *Stephania suberosa* Forman extract and ampicillin combination against ampicillin-resistant *Staphylococcus aureus*. *J Biomed Sci* 2014 2014/09/11;21(1):90.
3. Iqbal G, Faisal S, Khan S, Shams DF, Nadhman A. Photo-inactivation and efflux pump inhibition of methicillin resistant *Staphylococcus aureus* using thiolated cobalt doped ZnO nanoparticles. *J Photochem Photobiol B, Biol* 2019 2019/03/01/;192:141-6.
4. Saha R, Saha N, Donofrio RS, Bestervelt LL. Microbial siderophores: a mini review. *J Basic Microbiol* 2013;53(4):303-17.

5. Saranya J, Jone Kirubavathy S, Chitra S, Zarrouk A, Kalpana K, Lavanya K, et al. Tetradentate schiff base complexes of transition metals for antimicrobial activity. *Arab J Sci Eng* 2020 2020/06/01;45(6):4683-95.
6. Fayaz AM, Balaji K, Girilal M, Yadav R, Kalaichelvan PT, Venketesan R. Biogenic synthesis of silver nanoparticles and their synergistic effect with antibiotics: a study against gram-positive and gram-negative bacteria. *Nanotechnol Biol Med* 2010 2010/02/01;6(1):103-9.
7. Ye Q, Chen W, Huang H, Tang Y, Wang W, Meng F, et al. Iron and zinc ions, potent weapons against multidrug-resistant bacteria. *Appl Microbiol Biotechnol* 2020;104(12):5213-27.
8. Claudel M, Schwarte JV, Fromm KM. New antimicrobial strategies based on metal complexes. *Chemistry* 2020;2(4):849-99.
9. Hrioua A, Loudiki A, Farahi A, Laghrib F, Bakasse M, Lahrach S, et al. Complexation of amoxicillin by transition metals: Physico-chemical and antibacterial activity evaluation. *Bioelectrochemistry* 2021 2021/12/01;142:107936.
10. Santos JVD, Porto ALF, Cavalcanti IMF. Potential application of combined therapy with lectins as a therapeutic strategy for the treatment of bacterial infections. *Antibiotics* 2021;10(5):520.
11. Mgbeahuruike EE, Stålnacke M, Vuorela H, Holm Y. Antimicrobial and synergistic effects of commercial piperine and piperlongumine in combination with conventional antimicrobials. *Antibiotics* 2019;8(2):55.
12. Arias LS, Pessan JP, Vieira APM, Lima TMTd, Delbem ACB, Monteiro DR. Iron Oxide Nanoparticles for Biomedical Applications: A perspective on synthesis, drugs, antimicrobial activity, and toxicity. *Antibiotics* 2018;7(2):46.
13. Kopel P, Travnicek Z, Zboril R, Marek J. Synthesis, X-ray and Mossbauer study of iron(II) complexes with trithiocyanuric acid (ttcH(3)). The X-ray structures of Fe(bpy)(3) (ttcH) center dot 2bpy center dot 7H(2)O and Fe(phen)(3) (ttcH(2))(ClO4) center dot 2CH(3)OH center dot 2H(2)O. *Polyhedron [Article]* 2004 Sep;23(14):2193-202.
14. Ludwig C, Devidal J-L, Casey WH. The effect of different functional groups on the ligand-promoted dissolution of NiO and other oxide minerals. *Geochim Cosmochim Acta* 1996 1996/01/01;60(2):213-24.
15. Shirani M, Akbari-Adergani B, Rashidi Nodeh H, Shahabuddin S. Ultrasonication-facilitated synthesis of functionalized graphene oxide for ultrasound-assisted magnetic dispersive solid-phase extraction of amoxicillin, ampicillin, and penicillin. *G Mikrochim Acta* 2020;187.
16. von Wirén N, Khodr H, Hider RC. Hydroxylated phytosiderophore species possess an enhanced chelate stability and affinity for iron(III). *Plant Physiol* 2000;124(3):1149-58.
17. Nath H, Sharma P, Frontera A, Barcelo-Oliver M, Verma AK, Das J, et al. Phenanthroline-based Ni(II) coordination compounds involving unconventional discrete fumarate-water-nitrate clusters and energetically significant cooperative ternary  $\pi$ -stacked assemblies: Antiproliferative evaluation and theoretical studies. *J Mol Struct* 2022 2022/01/15;1248:131424.

18. Tipper DJ, Strominger JL. Mechanism of action of penicillins: a proposal based on their structural similarity to acyl-D-alanyl-D-alanine. *Proc Natl Acad Sci U.S.A* 1965;54(4):1133-41.
19. El-Gamel NEA. Metal chelates of ampicillin versus amoxicillin: synthesis, structural investigation, and biological studies. *J Coord Chem* 2010 2010/02/10;63(3):534-43.
20. Vazquez-Muñoz R, Meza-Villezcás A, Fournier PGJ, Soria-Castro E, Juárez-Moreno K, Gallego-Hernández AL, et al. Enhancement of antibiotics antimicrobial activity due to the silver nanoparticles impact on the cell membrane. *PLoS One* 2019;14(11):e0224904-e.
21. Panáček A, Smékalová M, Kilianová M, Pucek R, Bogdanová K, Večeřová R, et al. Strong and nonspecific synergistic antibacterial efficiency of antibiotics combined with silver nanoparticles at very low concentrations showing no cytotoxic effect. *Molecules* 2016;21(1):26.
22. Singh AV, Vyas V, Montani E, Cartelli D, Parazzoli D, Oldani A, et al. Investigation of in vitro cytotoxicity of the redox state of ionic iron in neuroblastoma cells. *J Neurosci Rural Pract* 2012;3(3):301-10.
23. Richardson DR, Lok HC. The nitric oxide–iron interplay in mammalian cells: Transport and storage of dinitrosyl iron complexes. *Biochim Biophys Acta Gen Subj* 2008 2008/04/01/;1780(4):638-51.
24. Padwal P, Bandyopadhyaya R, Mehra S. Polyacrylic acid-coated iron oxide nanoparticles for targeting drug resistance in mycobacteria. *Langmuir* 2014;30(50):15266-76.
25. Nallathamby PD, Lee KJ, Desai T, Xu X-HN. Study of the multidrug membrane transporter of single living *Pseudomonas aeruginosa* cells using size-dependent plasmonic nanoparticle optical probes. *Biochemistry* 2010;49(28):5942-53.
26. Hasani A, Madhi M, Gholizadeh P, Shahbazi Mojarrad J, Ahangarzadeh Rezaee M, Zarrini G, et al. Metal nanoparticles and consequences on multi-drug resistant bacteria: reviving their role. *SN Appl Sci* 2019 2019/03/25;1(4):360.
27. Banoee M, Seif S, Nazari ZE, Jafari-Fesharaki P, Shahverdi HR, Moballegh A, et al. ZnO nanoparticles enhanced antibacterial activity of ciprofloxacin against *Staphylococcus aureus* and *Escherichia coli*. *J Biomed Mater Res* 2010;93(2):557-61.
28. Singh N, Rajwade J, Paknikar KM. Transcriptome analysis of silver nanoparticles treated *Staphylococcus aureus* reveals potential targets for biofilm inhibition. *Colloids Surf B* 2019 2019/03/01/;175:487-97.
29. Wang R, Lai T-P, Gao P, Zhang H, Ho P-L, Woo PC-Y, et al. Bismuth antimicrobial drugs serve as broad-spectrum metallo- $\beta$ -lactamase inhibitors. *Nat Commun* 2018 2018/01/30;9(1):439.
30. Loss G, Simões PM, Valour F, Cortês MF, Gonzaga L, Bergot M, et al. *Staphylococcus aureus* small colony variants (scvs): news from a chronic prosthetic joint infection. *Front Cell Infect Microbiol* [Original Research] 2019 2019-October-22;9.
31. Jonsson I-M, Juuti JT, François P, AlMajidi R, Pietiäinen M, Girard M, et al. Inactivation of the Ecs ABC transporter of *Staphylococcus aureus* attenuates virulence by altering composition and function of bacterial wall. *PloS one* 2010;5(12):e14209-e.

32. Remy L, Carrière M, Derré-Bobillot A, Martini C, Sanguinetti M, Borezée-Durant E. The *Staphylococcus aureus* Opp1 ABC transporter imports nickel and cobalt in zinc-depleted conditions and contributes to virulence. Mol Microbiol 2013;87(4):730-43.

## Figures

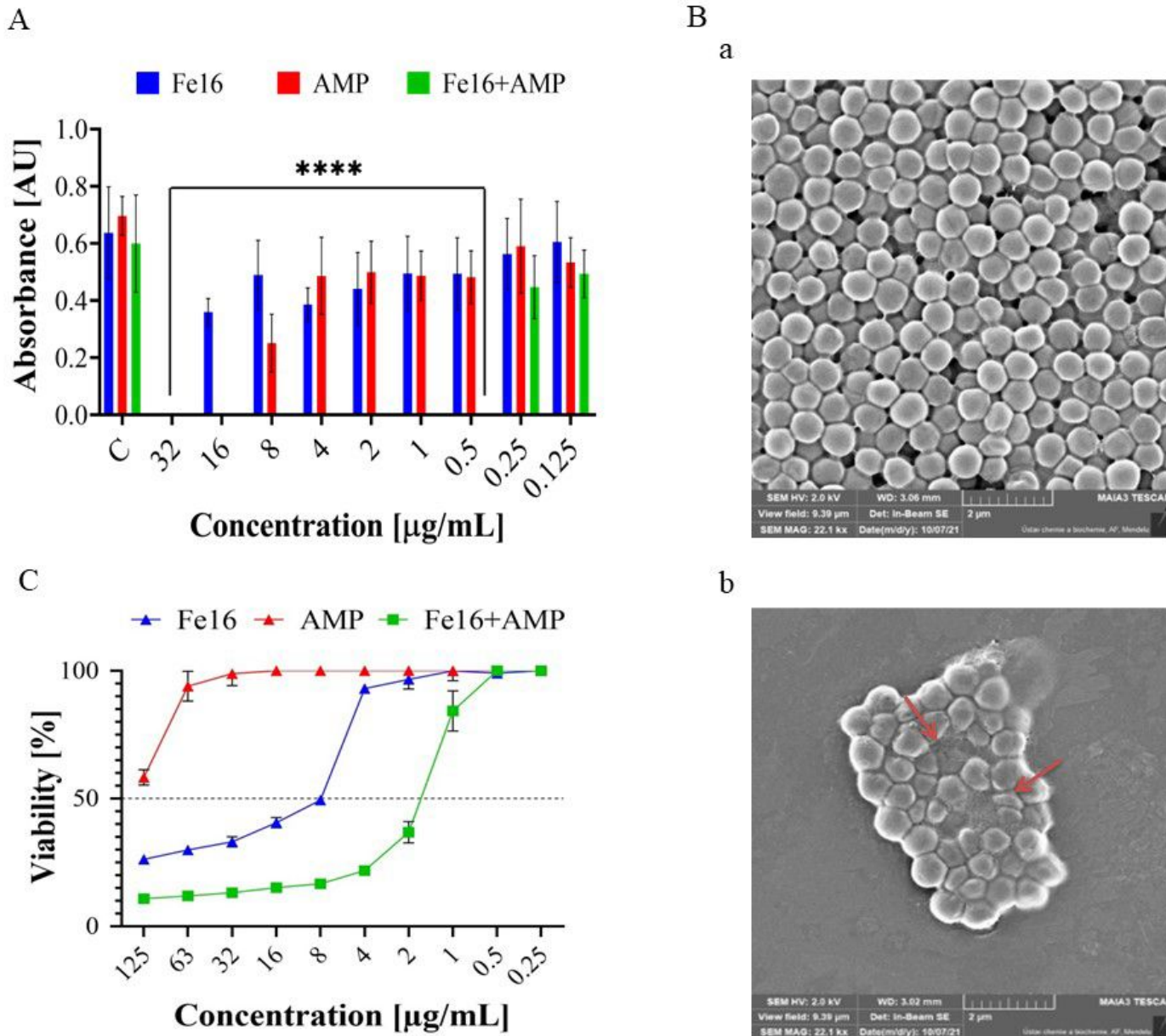


**Figure 1**

**A.** Representation of MIC values of Fe16, AMP, and Fe16+AMP on *S. aureus* at the various concentrations. Experiments were performed in biological triplicates. Significant changes of Fe16+AMP in comparison to control are marked with asterisk: \*\*\*\*p-value < 0.0001. **B.** External morphological changes of *S. aureus* after exposure to Fe16+AMP assessed by SEM. Figure a shows untreated *S. aureus* as a control and in figure b is *S. aureus* treated with Fe16+AMP at 0.25 µg/L. Red arrows indicate *S. aureus* morphological

changes. **C.** Cytotoxic effects of Fe16, AMP and Fe16+AMP at the different concentrations on the HaCaT keratinocyte cell line.

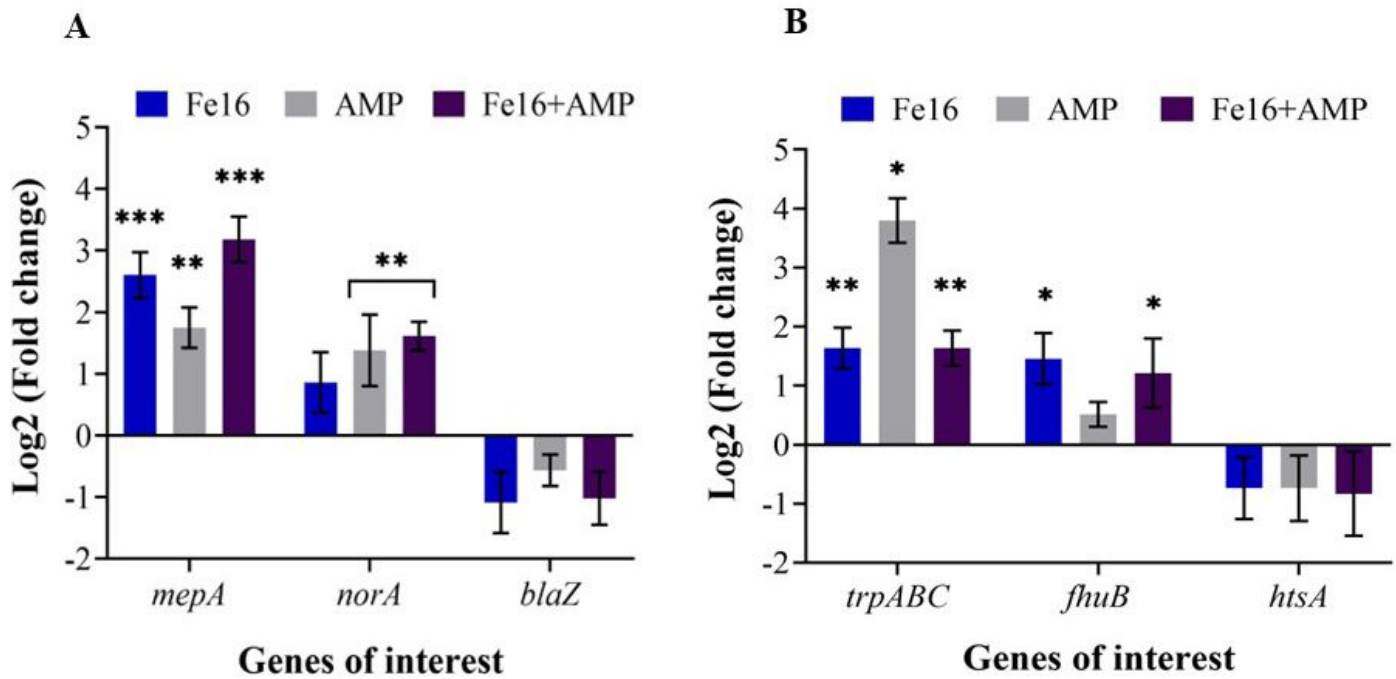


**Figure 2**

Gene expression a Log2 (fold change) of the ABC transporter family **(A)** and defense system of *S. aureus* after exposure to AMP, Fe16 and Fe16+AMP **(B)**. Significant changes of Fe16, AMP and Fe16+AMP in comparison to that of control are marked with asterisks: \*p-value < 0.05, \*\*p-value < 0.01, \*\*\*p-value < 0.001.

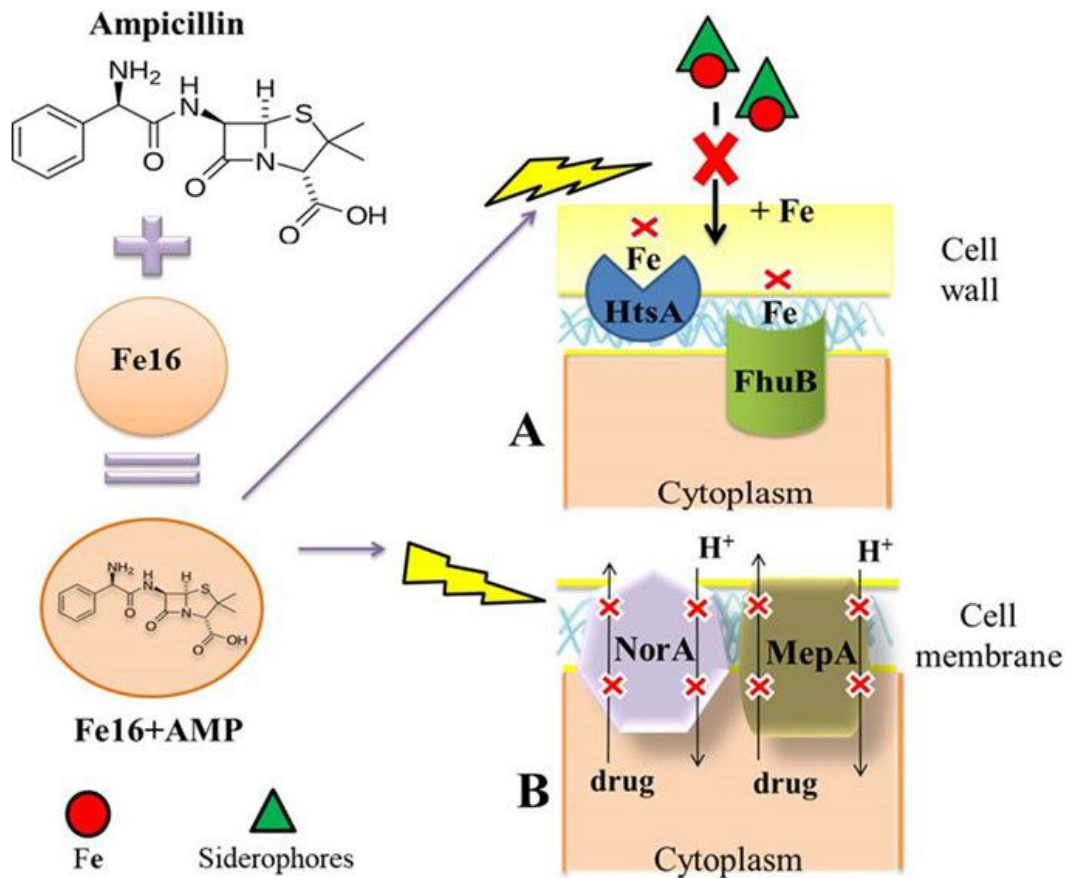


**Figure 3**

Mechanism of the antimicrobial effect of Fe16+AMP causing stress in *S. aureus* and disruption of function of efflux pumps and ABC transporters (C). **A.** NorA and MepA efflux pumps are not sufficient to push Fe16+AMP out of cells. **B.** Import of iron into cells, needed by *S. aureus* for growth and metabolism, is disrupted.

## Supplementary Files

This is a list of supplementary files associated with this preprint. Click to download.

- [Supplementarymanuscript.docx](#)